Reversible Chemochromic MoO_3 Nanoribbons through Zerovalent Metal Intercalation

Mengjing Wang and Kristie J. Koski*

Department of Chemistry, Brown University, Providence, Rhode Island 02912, United States

ABSTRACT Molybdenum trioxide (α-MoO_3) is a 2D layered oxide with use in electrochromic and photochromic devices owing to its ability to reversibly change color between transparent and light blue with electrochemical or hydrogen intercalation. Despite its significant application potential, MoO_3 performance is largely limited by the destructiveness of these intercalation techniques, insignificant coloration, and slow color response. We demonstrate a reversible chemochromic method, using intercalation of zerovalent metals into α-MoO_3 nanoribbons (Sn, ~2 at. %; Co, ~4 at. %), to chemically alter MoO_3 from transparent white to a deep blue indigo, resulting in enhanced coloration and chemically tunable optical properties. We present two strategies to reversibly tune the color response of MoO_3 nanoribbons. Chromism can be reversed (i) by complete oxidative deintercalation with hydrogen peroxide or iodine or (ii) through a temperature-driven disorder−order phase transition of the intercalated zerovalent metal.

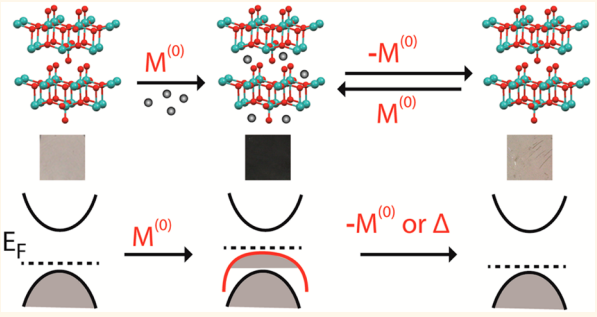

KEYWORDS: zerovalent intercalation · 2D materials · chemochromism · MoO_3 nanoribbons · electrochromism · photochromism

Materials that change color in response to an external stimulus (smart materials) are important in new technologies such as sensors, pregnancy tests, electrochromic and photochromic displays, mirrors, and smart windows.[1−3] Prominent among these materials, MoO_3 has been widely studied due to its extraordinary photochromic and electrochromic behaviors.[4−10] It has received renewed attention recently as a high-capacity Li battery cathode[11] and for catalyzing hydrogen evolution reactions.[12] MoO_3 is a two-dimensional, layered material with covalently bonded oxide layers separated by van der Waals gaps, which can serve as a host for guest intercalants. Both photochromism and electrochromism of MoO_3 are dictated by intercalation of hydrogen radicals, through photoreduction of water with UV light, or by electrochemical intercalation of lithium ions into the interlayer van der Waals gaps. Intercalated ions distort the lattice and add interband states into the wide band gap of MoO_3 (3.1 eV), enabling lower energy transitions and resulting in a light blue color.[4,13] The ionic nature of these intercalants, however, limits the amount of species uptake, either destabilizing the host structure or resulting in a reaction of the host + guest forming molybdenum bronze (A_xMoO_3, A = H or Li, Na, K) with an associated intervalence charge transfer between $Mo^{(5+)}$ and $Mo^{(6+)}$ ultimately limiting the color response of MoO_3.[10,13] Despite significant amounts of work, the chromic performance of MoO_3 is still largely limited by the destructiveness of ionic intercalation combined with subtle and slow coloration.[10,13−17]

Here, we use MoO_3 nanoribbons for their nanometer size, high crystal quality, sharp edges, and lack of surface ligands, which enable rapid intercalation of zerovalent metals coupled with significant color enhancement over bulk materials. We show that the limitations of ion intercalation can be overcome by intercalation of zerovalent metals, thus dramatically reducing destabilization of the host by the intercalant and allowing intercalation to very high densities, resulting in strong color changes without damaging the host. Recently, it has been shown that intercalation with zerovalent metals can result in enhanced electronic

* Address correspondence to koski@brown.edu.

Received for review January 15, 2015 and accepted March 3, 2015.

Published online March 03, 2015
10.1021/acsnano.5b00336

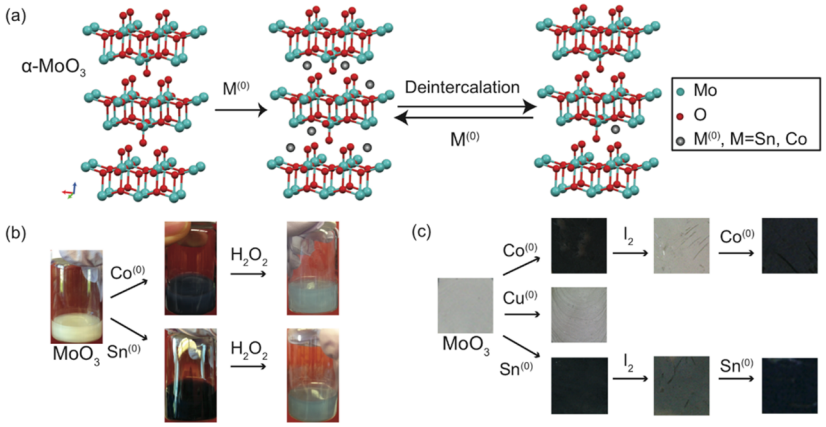

Figure 1. (a) Schematic illustration of reversible chemochromism through zerovalent metal intercalation and deintercalation into MoO_3 nanoribbons, which can be performed in solution or on a substrate. (b) MoO_3 undergoes a color transition when intercalated with $Co^{(0)}$ or $Sn^{(0)}$ metal, as observed in a solution of deionized water. Using H_2O_2 as a deintercalation reagent, zerovalent metal atoms can be removed from the nanoribbons, reverting the color to near-white. (c) Zerovalent metal atoms of $Co^{(0)}$ or $Sn^{(0)}$ can be intercalated into MoO_3 nanoribbons deposited on a fused silica substrate, resulting in a color change to deep indigo. I_2 can be used as a deintercalation reagent, reverting the nanoribbon color back to white. Intercalation with $Cu^{(0)}$ does not result in a color change of the MoO_3 nanoribbons.

transport and significantly enhanced transmission coincident with changes to the electronic structure of the 2D material.[18,19] We present a chemochromic method, using zerovalent metal intercalation of Co and Sn, to change the color of α-MoO_3 nanoribbons from white to an intense indigo color quite unlike the pale blue achievable with ionic intercalation. Intercalation of zerovalent Cu (13 at. %) does not force a chemochromic change in MoO_3 nanoribbons, revealing that the color change is not merely a process of chemical intercalation but suggestive of a complex interaction of structure and electronic properties. Further, we show that the color change can be reversed through two different methods. First, zerovalent metals can be deintercalated with oxidative removal of the intercalant through immersion of the nanoribbons in an oxidative solution such as hydrogen peroxide or iodine. Second, the color change can be reversed through a temperature-driven disorder–order phase transition. In both cases, the color change can be cycled repeatedly, highlighting the importance of minimizing chemical damage to the host crystal by using uncharged intercalants. These integrated strategies open up entirely new avenues of the control of materials at the atomic scale, enabling technologies such as new chemochromic smart windows and displays or temperature-dependent sensors.

RESULTS AND DISCUSSION

Reversible Chemochromism. α-MoO_3 is a layered material with an orthorhombic crystal structure (space group: *Pnma*; Figure 1a). α-MoO_3 nanoribbons, grown in the [001] direction, are synthesized using hydrothermal methods.[20] Nanoribbons can be tuned from a transparent-white color to a vivid deep-indigo through the chemical intercalation of zerovalent metals, Co and Sn (Figure 1a), into the van der Waals gap of the host crystal. Cobalt and tin were intercalated into MoO_3 nanoribbons using the methods of Koski *et al.*[19] Figure 1 shows the remarkable color change of MoO_3 nanoribbons both suspended in aqueous solution (Figure 1b) and concentrated on a transparent fused silica substrate (Figure 1c). The color change of the nanoribbons is striking especially compared with the simple photochromic response of MoO_3 nanoribbons exposed to UV light (Supporting Information; Figure S1). Intercalation of zerovalent copper into MoO_3 nanoribbons using the method of Koski *et al.*[19,21] achieves very high densities of intercalant concentration (up to 13 at. % Cu). This, however, does not result in a color change of the MoO_3 nanoribbons.[19,22] Nanoribbons remain white or slightly yellowed with intercalation of copper metal. The process of intercalation of zerovalent metals into the MoO_3 is therefore not the cause of the color change but is specific to the intercalant and the host–intercalant electronic and structural interaction. Intercalation of MoO_3 bulk powders with zerovalent Co, Sn, and Cu (Supporting Inforation, Figure S7) can be performed, yet powder morphology limits intercalation to approximately 1 at. %. Bulk powders also have distinctly less of a color change than MoO_3 nanoribbons.

Zerovalent metals can be removed through oxidative deintercalation of the (Co, Sn) metal layer by placing the nanoribbons in an oxidizing solution such as hydrogen peroxide at room temperature (Figure 1b) or under reflux in iodine in acetonitrile at 65 °C (Figure 1c). This procedure can be repeated reversibly, indefinitely tuning the chromic response of MoO_3 nanoribbons through zerovalent intercalation. Transmission electron microscopy (TEM) of the nanoribbons throughout the entire process shows that the nanoribbon morphology is not damaged or altered by repeated cycling (Sn-MoO_3 in Figure 2; Co-MoO_3 in

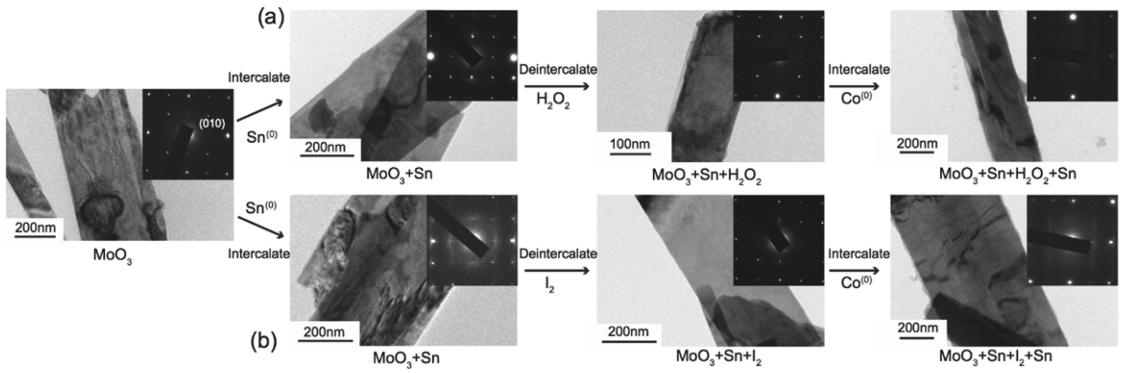

Figure 2. TEM images and selected area electron diffraction patterns of representative MoO_3 nanoribbons during intercalation, deintercalation, and reintercalation of Sn (a) using H_2O_2 and (b) I_2 for deintercalation. Nanoribbon morphology is preserved during multiple processing. SAED patterns (inset) show that crystallinity is preserved through processing. Changes in intensity to the (010) spot can be seen with intercalation and deintercalation.

Supporting Information Figure S2). Processing conditions are temperate enough to prevent destruction of the ribbons especially as compared to the electrochemical processes of intercalating and deintercalating Li^+, which tends to completely destroy sample morphology.[13] Selected area electron diffraction (SAED) patterns (Figure 2a, insets) show that the nanoribbons maintain crystallinity. Subtle changes in the intensity of {010} and {001} spots, however, occur with intercalation and deintercalation. These spots are forbidden in an ideal MoO_3 crystal and indicate, among other things, the presence and degree of crystallographic ordering of intercalant species.[22] These spots appear even in the pristine materials due in part to the presence of intercalated H_2O remaining in the van der Waals gap from growth.

Most of the zerovalent metal intercalant can be removed from the host MoO_3 nanoribbons through oxidative deintercalation. Energy dispersive X-ray spectroscopy (EDX) was used to determine the chemical composition and intercalant percentage throughout the process (Figure 3) from an average atomic percent of intercalant of 5−10 nanoribbons. In a typical intercalation, ~4 at. % of Co and 2 at. % of Sn are intercalated into the nanoribbons. With oxidative deintercalation, EDX spectra show near-complete removal of intercalant with some dependence upon deintercalating solvent (Supporting Information, Table S1). Less than one atomic percent of Co or Sn is detected through EDX after oxidative deintercalation. Figure 3a,b reveals that the atomic percent intercalant Sn to MoO_3 host could be deintercalated from $1.3 \pm 0.2\%$ to $0.09 \pm 0.08\%$ after hydrogen peroxide treatment and from $1.8 \pm 0.6\%$ to $0.2 \pm 0.05\%$ after I_2 treatment. Figure 3c,d shows that the atomic percent of intercalated cobalt to MoO_3 host could be deintercalated from $1.3 \pm 0.3\%$ to $0.08 \pm 0.02\%$ after H_2O_2 treatment and from $1.3 \pm 0.4\%$ to $0.04 \pm 0.01\%$ after I_2 treatment (Supporting Information, Table S1). The strength of the oxidative potential plays an enormous role in the removal of the intercalant from the host. The subtle difference of the

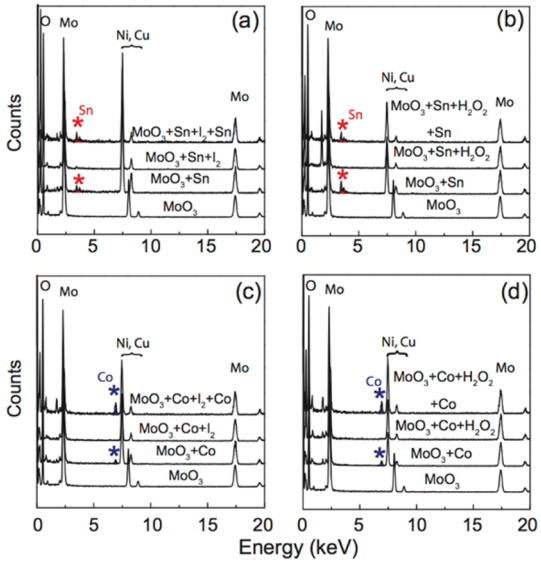

Figure 3. Energy dispersive X-ray spectra showing elemental composition after each intercalation, deintercalation, and reintercalation show reversible, complete removal and reinsertion of the zerovalent $Co^{(0)}$ and $Sn^{(0)}$ metal atoms from the MoO_3 nanoribbon host. Deintercalation of Sn from MoO_3 (red asterisks) using (a) I_2 and (b) H_2O_2 as oxidative reagents. Deintercalation of Co from MoO_3 (blue asterisks) using (c) I_2 and (d) H_2O_2 for deintercalation. Ni or Cu signal is from the TEM grids.

effectiveness of deintercalation, as found in EDX, between I_2 and H_2O_2 as oxidative reagents is in agreement with the relative oxidation potential. $\varphi_{H2O2/H2O} = +1.77$ V, $\varphi_{I2/I^-} = +0.535$ V of these reagents.[23] H_2O_2 is a stronger oxidative reagent and can deintercalate Sn and Co more effectively than iodine. Similarly, Co-MoO_3 is easier to deintercalate than Sn using either hydrogen peroxide or iodine simply because Sn has a weaker propensity to be oxidized.[23]

Figure 4 shows X-ray diffraction (XRD) data of MoO_3, $Sn_{0.07}MoO_3$, and $Co_{0.05}MoO_3$ after intercalation, deintercalation, and reintercalation. Insets are the *a* lattice constant, which corresponds to the direction of expansion or contraction of the van der Waals gap, calculated from the position of (2*n* 0 0) peaks after each step

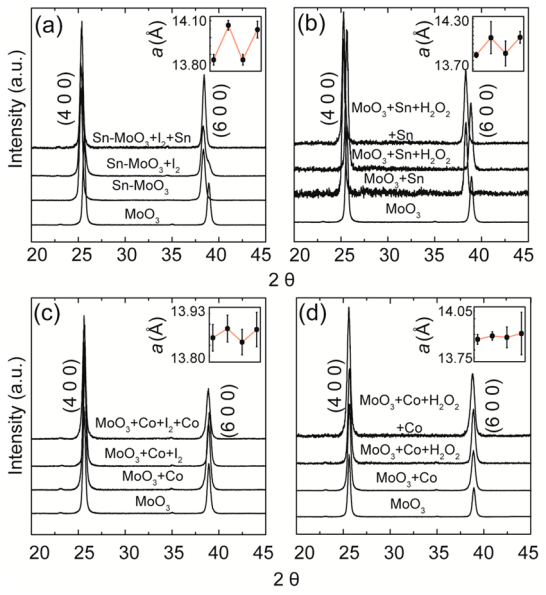

Figure 4. XRD of MoO_3 before intercalation, intercalated, deintercalated, and reintercalated. Insets are values of the *a* lattice constant, which corresponds with the direction of expansion or contraction of the van der Waals gap of the 2D layers after each step. Note the near-complete reproducibility of intercalation and deintercalation of zerovalent metals from the host using this strategy. (a) Iodine deintercalation of Sn from MoO_3, (b) H_2O_2 deintercalation of Sn from MoO_3, (c) iodine deintercalation of Co from MoO_3, (d) H_2O_2 deintercalation of Co from MoO_3.

(Supporting Information, Table S1). The van der Waals gap shows a large increase following intercalation of metal atoms (Co, Sn), which is subsequently recovered after oxidative deintercalation. When I_2 was used as an oxidative reagent to remove tin atoms (Figure 4a), a peak splitting of the (2*n* 0 0) is seen, with one peak corresponding to the intercalated Sn-MoO_3 and another to the original MoO_3 peak, consistent with EDX data that show that not quite 100% of the Sn intercalant is removed using I_2. Expansion of the host depends on the concentration of intercalant as well as the nature and relative size of the zerovalent atomic species. For example, the change of lattice constant, *a*, in Co-MoO_3 is less than that of Sn-MoO_3, surely due in part to the size of the intercalated metal atom species and difference in bonding patterns, as evidenced by the differences in the SAED relative spot intensities.

Reversible Chemochromism/Thermochromism. Intercalated metals occupy sites in the van der Waals gap that are typically disordered relative to the host structure until the intercalant concentration reaches above 10−15 atomic percent.[19,21,22,24] Intercalant ordering can be induced through a temperature-driven, disorder−order phase transition. Such disorder−order phase transitions are well established as an intrinsic behavior property of guests in intercalation materials.[19,25−27] In Co- and Sn-intercalated MoO_3 nanoribbons, heating to 180 and 150 °C in air in 20 °C steps starting from 20 °C with 3 min of stabilization time, respectively, induces ordering of the intercalant and is accompanied by a color change from indigo back to a transparent white. Figure 5a presents a schematic. A second intercalation of Co or Sn (Figure 5c,d) reverts the color to deep indigo and, with subsequent heating, back to white again. This can be performed until a maximum capacity of intercalant is reached in the host lattice. Colors are preserved upon cooling and storage for several months. Nanoribbon morphology is also preserved throughout intercalation and heating (Supporting Information, Figures S4 and S5). A control sample of MoO_3 nanoribbons deposited on a fused silica substrate (Figure 5b) shows no color change with heating to above 300 °C.

EDX spectra (Supporting Information, Figure S6) show that the maximum atomic percent of cobalt in MoO_3 is reached at an average of 4.2% ($Co_{0.17}MoO_3$), and the maximum ratio of tin in MoO_3 is reached at 1.9% ($Sn_{0.08}MoO_3$). For the experiments presented here, MoO_3 intercalated with cobalt underwent two cycles before maximum capacity was reached, while samples intercalated with tin could undergo six cycles (Figure 5). Reducing intercalant by simply decreasing the intercalation time or concentration of intercalant precursor can be used to increase the overall number of chemochromic−thermochromic cycles.

The lattice constants of intercalated MoO_3 were measured using X-ray diffraction with *in situ* heating in air to 430 °C (Figure 6). Figure 6 shows the diffraction patterns from MoO_3, $Co_{0.15}MoO_3$, and $Sn_{0.006}MoO_3$. α-MoO_3 has an orthorhombic crystal structure with lattice constants $a = 13.86 \pm 0.01$ Å, $b = 3.70 \pm 0.01$ Å, and $c = 3.96 \pm 0.01$ Å (unit cell volume 203.1 Å^3). Intercalation of 13 at. % of Cu gives values of $a = 13.84$ Å, $b = 3.60$ Å, and $c = 3.95$ Å (unit cell volume 196.8 Å^3),[22] which is a notable contraction of the volume of the host lattice when compared with Co and Sn. Intercalation with 3.8 at. % Co gives values of $a = 13.95$ Å, $b = 3.60$ Å, and $c = 4.01$ Å (unit cell volume 201.3 Å^3) and with 0.15% of Sn values of $a = 13.93$ Å, $b = 3.58$ Å, and $c = 4.01$ Å (unit cell volume 199.98 Å^3). The lattice, as a whole, can contract with lower concentrations of intercalant as noted previously.[19,28] Peaks are labeled according to the *Pnma* space group (which is physically equivalent to the *Pbnm* convention used by some authors[4,20]), where *a* is the axis corresponding to changes in the van der Waals spacing. Co and Sn lead to a notable increase in the *a* lattice constant, which is the direction of expansion of the van der Waals gap; Cu intercalation leads instead to a decrease in the *a* lattice constant, indicating contraction of the van der Waals gap. Lattice constants (Figure 6d−f) show noticeable change with heating of intercalated samples that directly correlates with the change of sample color. Temperature regions are shaded to indicate where the intercalated MoO_3 samples revert from blue to white with heating. Within the precision of the measurement, the pure and the Sn-intercalated materials are almost

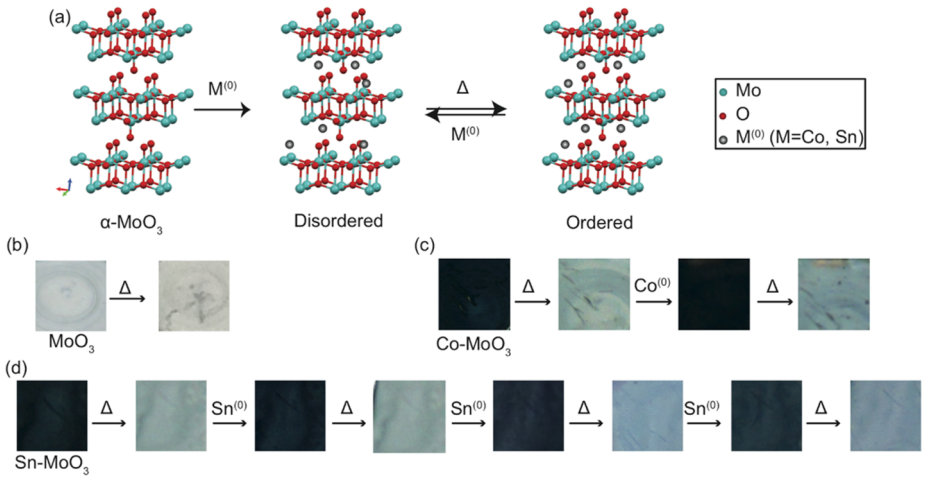

Figure 5. (a) Schematic of the temperature-induced, reversible color change of MoO_3 through a temperature-driven, disorder−order phase transitions of zerovalent $Co^{(0)}$ and $Sn^{(0)}$ intercalated into MoO_3 nanoribbons. (b) Control MoO_3 nanoribbons deposited on a fused silica substrate remain white with heating to 200 °C in air. (c) MoO_3 nanoribbons deposited on a substrate undergo a color change with intercalation of $Co^{(0)}$. With heating to 200 °C in air, the intercalant undergoes a disorder−order transition resulting in a color change to white. More $Co^{(0)}$ can be intercalated into MoO_3, reverting the color back to blue, and with further heating the color changed to white. This can be repeated numerous times until a maximum intercalant capacity is reached in the host. (d) This same intercalation and annealing procedure can be performed cyclically with $Sn^{(0)}$-intercalated MoO_3 nanoribbons as well.

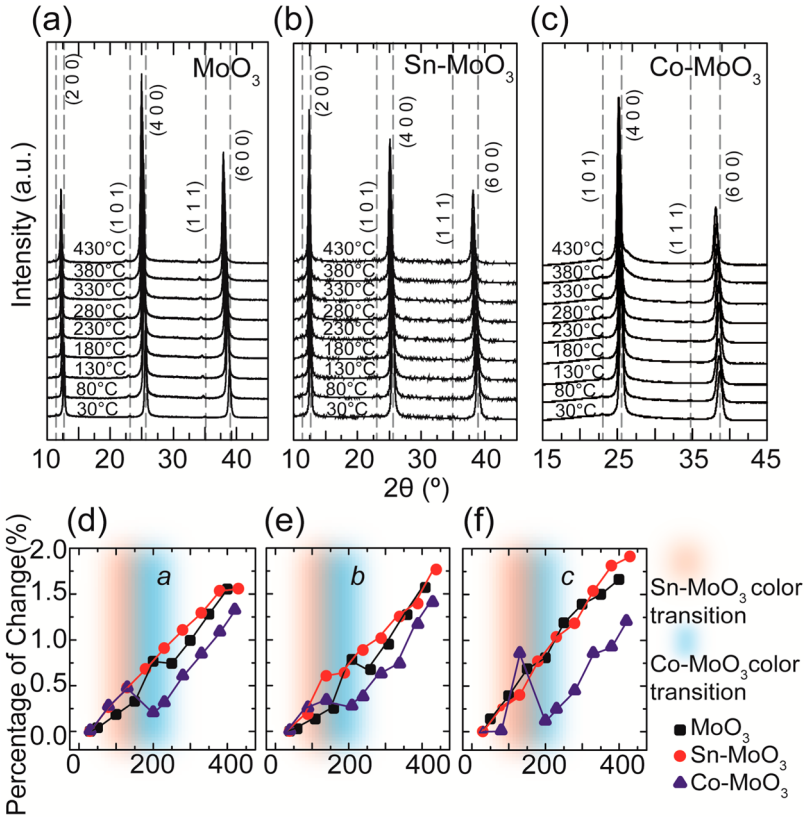

Figure 6. *In situ* XRD of (a) MoO_3 nanoribbon control, (b) MoO_3 intercalated with Sn, and (c) intercalated with Co. (d−f) Percent change of lattice constants *a*, *b*, and *c* of MoO_3 and intercalated MoO_3 as a function of temperature. The red area represents the color-transition temperature range of Sn-MoO_3; the blue region represents the color transition of Co-MoO_3. Some small structural change is observed in the host through annealing, which correlates with a disorder−order transition of the guest intercalant characteristic of intercalated layered materials. Error bars are within the plot symbol.

indistinguishable, both expanding nearly linearly and isotropically with temperature, with nothing much happening at the Sn color transition, while the Co shows a reduction in all three lattice constants at the temperature. The larger changes observed in cobalt intercalated MoO_3 is attributed to the larger concentration of

intercalant and thus greater interaction of the guest and host. Due to the low intercalant concentration, superlattice peaks are not observed in any of the diffraction data.

The changes observed with diffraction and correlated with the color change are consistent with a structural change in the guest + host system.[22] Figure 7 presents a control SAED pattern of MoO_3 nanoribbons (Figure 7a,b) and $Sn_{0.006}MoO_3$ nanoribbons (Figure 7c,d) heated in air up to 200 °C with 20 °C steps and 5 min of stabilization time at each step. SAED patterns of $Sn_{0.006}MoO_3$ and $Co_{0.15}MoO_3$ (Supporting Information, Figure S9), measured with TEM after heating *ex situ* in air using the same heating method in air, present evidence for ordering of the guest within the lattice. Electron diffraction patterns are zero-order Laue zone (ZOLZ) patterns at or near a [100] zone axis, consisting of Bragg spots with indices (0*kl*). In an ideal MoO_3 crystal structure, the {010} and {001} spots (and indeed all spots with $h = 0$ and $k+l$ being an odd integer) are forbidden both kinematically and dynamically and should not appear in the SAED patterns. Heating of the MoO_3 nanoribbon control shows little to no change in the spot intensity or SAED pattern. Heating of the $Sn_{0.006}MoO_3$ nanoribbons results in a disorder−order transition of the intercalant; diffraction shows changes in spot intensities and also in disorder, most obviously in the (010) and (001) spots, which are quite diffuse (indicative of disorder) in the unannealed state. Annealing $Co_{0.15}MoO_3$ strengthens the intensity of the forbidden spots (Supporting Information, Figure S8). The presence of strong forbidden spots even after annealing indicates that that the annealed structure is of lower symmetry than the pure MoO_3 crystal, while the strengthening of these spots during annealing indicates that the annealing itself facilitates the symmetry breaking; the material has relaxed into a new kind of order distinct from the original crystal structure. Combining the XRD and SAED results, it appears that the two materials both undergo disorder−order transitions associated with the color change from indigo to white but that these transitions are very different in detail. The transition in the Sn-intercalated material involves a sharpening of existing spots and negligible change in the lattice constants, while in the Co-intercalated material the lattice contracts as the symmetry is broken during the transformation. However, in both cases it appears that the relaxation of the intercalant into more stable states largely eliminates the color centers produced by the initial intercalation into, presumably, a mix of higher energy interstitial sites. Heating nanoribbons *in situ* in a vacuum in a TEM, with 20 °C steps from 20 to 380 °C with 3 min of stabilization at each step followed by slow cooling, results in a large variety of superlattice disorder−order transitions different from those observed during heating in air (Supporting Information, Figures S10, S11).

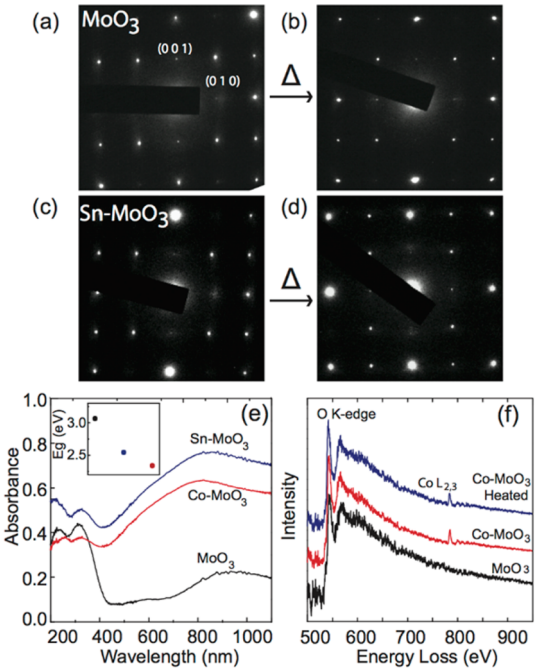

Figure 7. Thermochromically induced color response of zerovalent intercalated MoO_3 is accompanied by a structural change of the guest atoms within the lattice determined through SAED and showing no change in oxidation state of the host or intercalant through EELS. Electron diffraction of Sn-MoO_3 shows evidence of a disorder−order transition of the guest shown through a change in the lattice spot intensity, such as the (010). SAED patterns of (a) MoO_3 and (b) MoO_3 annealed at 350 °C in air; SAED patterns of (c) Sn-MoO_3 and (d) Sn-MoO_3 annealed at 350 °C in air. (e) UV−visible absorbance of MoO_3 (black line), Co-MoO_3 (red line), and Sn-MoO_3 (blue line). Note the substantial absorption change accomplished by intercalation of zerovalent metals. The band gap calculated from these data is shown as an inset, demonstrating tunable band gap through zerovalent intercalation. (f) EELS spectroscopy of the O K edge and Co $L_{2,3}$ edges. The Co $L_{2,3}$ ratio does not change with annealing, indicating that there is no change in oxidation state accompanied by the color response.

The coloration efficiency of intercalation of zerovalent metals in MoO_3 can be quantified through diffuse reflectance ultraviolet−visible (UV−vis) absorbance measurements of MoO_3 and MoO_3 intercalated with cobalt and tin (Figure 7e; Supporting Information, Figure S12). UV−vis measurements reveal remarkably stronger absorbance of intercalated samples throughout the entire range measured. The UV−vis of the pristine nanoribbons is the photochromic response seen in MoO_3. The longer wavelength region (800−900 nm) shows an almost 3-fold increase in absorption compared to that of untreated MoO_3 nanoribbons. This is consistent with the remarkable dark indigo-blue color of MoO_3 after intercalation of Co or Sn. The UV−vis absorbance spectrum also reveals the large coloration efficiency enhancement of our intercalation method. The calculated band gap from the UV−vis data is shown as an inset in Figure 7e (further details in Supporting Information Figures S12 and S13). The band-gap energy decreases

from 3.1 eV for MoO_3 to 2.5 eV for Sn-MoO_3 and 2.3 eV for Co-MoO_3.

Electron energy loss spectroscopy (EELS) is a powerful technique to provide information about the electronic environment surrounding an atomic species, to identify the oxidation state of an intercalated transition metal based on the near-edge fine structure information, and to reveal information about the electronic excitations of the material. Low-loss EELS (Supporting Information, Figure S14) shows similar peaks consistent with electronic edges seen in the UV−vis spectra, although the signal-to-background ratio is a problem due to overlap with the tails of the zero-loss peak. EELS fine structure can be used to identify the oxidation state of the intercalant and host to identify any mutual oxidation state changes or electron interaction. Negligible charge transfer is found with annealing as determined through EELS fine structure of the O K edge and Co L_3/L_2 edge from a single nanoribbon (Figure 7f). No changes were found in oxidation state and electronic environment before and after intercalation and heating. These data were collected on the same nanoribbon heated *ex situ* and located on a TEM finder grid throughout the entire experiment. The oxygen K edge shows no change with intercalation or heating, revealing that the intercalated metal has little to no direct electronic interaction, such as bonding, with the oxygen atoms, of the host MoO_3. The ratio of the cobalt L_3/L_2 edges before and after intercalation remains the same. It does not change with heating, which means that the electronic interaction of the cobalt and oxygen is not altered throughout the process. Copper intercalation into MoO_3, as investigated previously using EELS,[22,24] shows strong interaction of the copper guest and host MoO_3, although the MoO_3 nanoribbon color remains unchanged with intercalation.

From these results and analysis, we can propose an explanation for the chromic behavior and reversible processes based on the coupled behavior of structural and electronic properties. Intercalated, disordered zerovalent atoms perform two functions in MoO_3. First, they can distort the host structure with intercalation, particularly through expansion of the van der Waals gap, which can create localized electronic states associated distortion.[4] This point is supported from the comparison of the *a* lattice constant expansion or contraction after intercalation of Co, Sn, and Cu atoms. Second, beyond modifying existing states, the intercalants can also add discrete electronic interband states of their own between the valence band and conduction band, which decreases the effective band gap and results in a striking blue-indigo color, as revealed in the color response of the Sn- and Co-MoO_3 intercalated samples. The addition of interband states relies heavily on the electronic and structural interaction between host and guest. Very recent computational results further support this argument. Huang *et al.*[4] found that n-type electronic doping, which would be the type of doping provided by zerovalent metal intercalation, can lead to a lattice distortion and a corresponding reduction in the band gap. We have shown that it is possible to induce a color change through zerovalent intercalation and reverse the color change with removal of the intercalant. Before intercalation, MoO_3 is an insulator, which has a large band gap and absorbs almost no UV−visible light; thus it is colorless. After intercalation with zerovalent metals, the guest metal atoms (Co and Sn) act as a color center for the MoO_3, distorting the host lattice as observed in the XRD lattice constants. This can be seen in the strain induced in the crystal lattice with intercalation from the SAED patterns showing intense forbidden reflection and subsequent release with heating. Intercalation of zerovalent copper, which does not yield a color change, results in a decrease in the layer spacing in the MoO_3 lattice; intercalation of Cu also results in interaction with the host MoO_3 with an oxidation state change of the zerovalent copper.[22,24] When the sample is heated above a transition point, intercalants in the van der Waals gap undergo a disorder−order phase transition; the color centers disappear. There is an absorption change accompanied by a disorder−order phase transition, yet there is no change in the oxidation state. With heating, the color response goes away as the lattice distortion decreases coincident with the disorder−order phase transition.

CONCLUSIONS

These novel chemochromic methods show strong potential for new chemochromic smart windows, chemochromic displays, and color-changing temperature sensors, which may have use in other ceramics applications such as coatings. This work also serves as the first demonstration of deintercalation of a chemically intercalated zerovalent metal from a host lattice, thus enabling wider applicability of zerovalent intercalation in 2D hosts.

MATERIALS AND METHODS

Preparation of α-MoO_3. α-MoO_3 nanoribbons are synthesized using the hydrothermal method of Li *et al.*[20] Synthesized nanoribbons are approximately 10 nm in thickness with 200 nm width and 1000 nm length.[20,22] Approximately 0.1 mL of MoO_3 nanobelt solution was either (i) drop-cast onto fused silica substrates and heated at 105 °C for 4 h to evaporate all water or (ii) left in DI water for solution-based intercalation.

Intercalation of Zerovalent Metals. Zerovalent metals of Co, Sn, and Cu were intercalated into the van der Waals gap using the methods of Koski *et al.*[19,21] For Sn intercalation, the MoO_3 substrate was placed in a 10 mM solution of $SnCl_2$ and

100 mM tartaric acid in acetone just under reflux for 1 h.[19] The color change can be seen visibly in solution in less than 5 min. Intercalation of zerovalent Sn proceeds *via* the disproportionation redox reaction of Sn(II). Zerovalent cobalt was intercalated by the carbonyl decomposition of dicobalt octacarbonyl.[19] Dropwise, a solution of 0.01 g of dicobalt octacarbonyl dissolved in 3 mL of air-free acetone was added to the substrate in 8 mL of air-free acetone at 55 °C in an inert N_2 environment over the time period of 1 h. A substrate of the nanoribbons was placed into a solution containing 5 mL of acetone and 0.13 g of tetrakis(acetonitrile)copper(I) hexafluorophosphate; the solution was kept under reflux for 4 h. Intercalated substrates were rinsed repeatedly with acetone and ethanol following intercalation. Intercalation was confirmed through a color change of the α-MoO_3 substrate. Intercalant concentration was determined with TEM EDX.

Deintercalation-Driven Reversible Chromism. For chemical deintercalation using hydrogen peroxide, 1 mL of 30% H_2O_2 solution was added to 5 mL of deionized water together with dried intercalated MoO_3. The sample was stirred at room temperature for 1 h. Deintercalated MoO_3 were washed with acetone and dried. For chemical deintercalation using iodine, intercalated MoO_3 on a substrate was placed in 5 mL of acetonitrile dissolved with 0.1 g of I_2 in a round-bottom flask at 60 °C for 3 days. The sample was removed and washed with dry acetone three times. Deintercalation was identified by a color change from blue to white and confirmed through TEM EDX.

Temperature-Driven Reversible Chromism. Temperature-dependent chromism of intercalated α-MoO_3 nanoribbons was studied *ex situ* on a heating stage, in 20 °C steps from 20 to 380 °C with 5 min of stabilization time. Corresponding structural properties of intercalated MoO_3 were studied using *in situ* XRD, in 50 °C steps from 30 to 380 °C with 5 min of stabilization time, and *in situ* TEM and SAED heating experiments, under vacuum with a GATAN 628 single tilt heating holder, in 20 °C steps from 20 to 380 °C with 3 min of stabilization time.

Characterization. *In situ* TEM images, SAED, EDX, and EELS spectra were collected with a JEOL 2100F at 200 keV. X-ray diffraction data were acquired on a Bruker D8 Discover diffractometer with a copper source ($K_{\alpha1}$ = 1.5406 Å, $K_{\alpha2}$ = 1.54439 Å). Lattice parameters were determined through Rietveld refinement with Maud and confirmed through calculation of lattice spacing from peak positions. UV−vis measurements were collected using an Evolution 220LC UV−vis SPEC with an integrating sphere from Thermo Fisher.

Conflict of Interest: The authors declare no competing financial interest.

Supporting Information Available: Optical images of unintercalated MoO_3 exposed to UV light; TEM images of MoO_3 before and after intercalation and heating; tables of lattice constants and intercalation atomic percentages determined through XRD and EDX; *in situ* TEM heating SAED patterns; Tauc plot to extract the energy band gaps; and low-loss EELS are provided. This material is available free of charge *via* the Internet at http://pubs.acs.org.

Acknowledgment. K.J.K. gratefully acknowledges support through Brown University startup funds.

REFERENCES AND NOTES

1. Granqvist, C.-G. Electrochromic Materials: Out of A Niche. *Nat. Mater.* **2006**, *5*, 89–90.
2. Granqvist, C. Electrochromism and Smart Window Design. *Solid State Ionics* **1992**, *53*, 479–489.
3. Lampert, C. M. Chromogenic Smart Materials. *Mater. Today* **2004**, *7*, 28–35.
4. Huang, P.-R.; He, Y.; Cao, C.; Lu, Z.-H. Impact of Lattice Distortion and Electron Doping on α-MoO_3 Electronic Structure. *Sci. Rep.* **2014**, *4*, 7131.
5. Brezesinski, T.; Wang, J.; Tolbert, S. H.; Dunn, B. Ordered Mesoporous α-MoO_3 with Iso-oriented Nanocrystalline Walls for Thin-Film Pseudocapacitors. *Nat. Mater.* **2010**, *9*, 146–151.
6. Arnoldussen, T. C. Electrochromism and Photochromism in MoO_3 Films. *J. Electrochem. Soc.* **1976**, *123*, 527–531.
7. Balendhran, S.; Walia, S.; Nili, H.; Ou, J. Z.; Zhuiykov, S.; Kaner, R. B.; Sriram, S.; Bhaskaran, M.; Kalantar-zadeh, K. Two-Dimensional Molybdenum Trioxide and Dichalcogenides. *Adv. Funct. Mater.* **2013**, *23*, 3952–3970.
8. Balendhran, S.; Deng, J.; Ou, J. Z.; Walia, S.; Scott, J.; Tang, J.; Wang, K. L.; Field, M. R.; Russo, S.; Zhuiykov, S. Enhanced Charge Carrier Mobility in Two-Dimensional High Dielectric Molybdenum Oxide. *Adv. Mater.* **2013**, *25*, 109–114.
9. Xiang, D.; Han, C.; Zhang, J.; Chen, W. Gap States Assisted MoO_3 Nanobelt Photodetector with Wide Spectrum Response. *Sci. Rep.* **2014**, *4*, 4891.
10. He, T.; Yao, J. Photochromism of Molybdenum Oxide. *J. Photochem. Photobiol. C* **2003**, *4*, 125–143.
11. Meduri, P.; Clark, E.; Kim, J. H.; Dayalan, E.; Sumanasekera, G. U.; Sunkara, M. K. MoO_{3-x} Nanowire Arrays As Stable and High-Capacity Anodes for Lithium Ion Batteries. *Nano Lett.* **2012**, *12*, 1784–1788.
12. Chen, Z.; Cummins, D.; Reinecke, B. N.; Clark, E.; Sunkara, M. K.; Jaramillo, T. F. Core−Shell MoO_3−MoS_2 Nanowires for Hydrogen Evolution: A Functional Design for Electrocatalytic Materials. *Nano Lett.* **2011**, *11*, 4168–4175.
13. Julien, C.; Pereira-Ramos, J.-P.; Momchilov, A. *New Trends in Intercalation Compounds for Energy Storage*; Springer, 2002; Vol. 61.
14. Surovoi, E.; Eremeeva, G. Thermal Transformations in In-MoO_3 Nanofilms. *Inorg. Mater.* **2013**, *49*, 390–394.
15. Yao, J.; Yang, Y.; Loo, B. Enhancement of Photochromism and Electrochromism in MoO_3/Au and MoO_3/Pt Thin Films. *J. Phys. Chem. B* **1998**, *102*, 1856–1860.
16. He, T.; Ma, Y.; Cao, Y.; Jiang, P.; Zhang, X.; Yang, W.; Yao, J. Enhancement Effect of Gold Nanoparticles on the UV-Light Photochromism of Molybdenum Trioxide Thin Films. *Langmuir* **2001**, *17*, 8024–8027.
17. Yang, Y.; Cao, Y.; Loo, B.; Yao, J. Microstructures of Electrochromic MoO_3 Thin Films Colored by Injection of Different Cations. *J. Phys. Chem. B* **1998**, *102*, 9392–9396.
18. Yao, J.; Koski, K. J.; Luo, W.; Cha, J. J.; Hu, L.; Kong, D.; Narasimhan, V. K.; Huo, K.; Cui, Y. Optical Transmission Enhancement Through Chemically Tuned Two-Dimensional Bismuth Chalcogenide Nanoplates. *Nat. Commun.* **2014**, 55670.
19. Koski, K. J.; Wessells, C. D.; Reed, B. W.; Cha, J. J.; Kong, D.; Cui, Y. Chemical Intercalation of Zerovalent Metals into 2D Layered Bi_2Se_3 Nanoribbons. *J. Am. Chem. Soc.* **2012**, *134*, 13773–13779.
20. Li, G.; Jiang, L.; Pang, S.; Peng, H.; Zhang, Z. Molybdenum Trioxide Nanostructures: The Evolution from Helical Nanosheets to Crosslike Nanoflowers to Nanobelts. *J. Phys. Chem. B* **2006**, *110*, 24472–24475.
21. Koski, K. J.; Cha, J. J.; Reed, B. W.; Wessells, C. D.; Kong, D.; Cui, Y. High-Density Chemical Intercalation of Zero-valent Copper into Bi_2Se_3 Nanoribbons. *J. Am. Chem. Soc.* **2012**, *134*, 7584–7587.
22. Reed, B. W.; Chung, F. R.; Wang, M.; LaGrange, T.; Koski, K. J. Temperature-Driven Disorder−Order Transitions in 2D Copper-Intercalated MoO_3 Revealed Using Dynamic Transmission Electron Microscopy. *2D Mater.* **2014**, *1*, 035001.
23. Lide, D. R. *CRC Handbook of Chemistry and Physics*; CRC Press, 2004.
24. Motter, J. P.; Koski, K. J.; Cui, Y. General Strategy for Zero-Valent Intercalation into Two-Dimensional Layered Nanomaterials. *Chem. Mater.* **2014**, *26*, 2313–2317.
25. Dresselhaus, M. *Intercalation in Layered Materials*; Dresselhaus, M. S., Ed.; Plenum Press: New York, 1986.
26. Lévy, F. *Intercalated Layered Materials*; Springer, 1979.
27. Müller-Warmuth, W. *Progress in Intercalation Research*; Springer, 1994; Vol. 17.
28. Powell, A. Intercalation Compounds of Low-Dimensional Transition Metal Chalcogenides. *Annu. Rep. Prog. Chem., Sect. C: Phys. Chem.* **1993**, *90*, 177–213.